NAB1 Is an RNA Binding Protein Involved in the Light-Regulated Differential Expression of the Light-Harvesting Antenna of *Chlamydomonas reinhardtii*

Jan H. Mussgnug,[a] Lutz Wobbe,[a] Ingolf Elles,[b] Christina Claus,[a] Mary Hamilton,[c] Andreas Fink,[d] Uwe Kahmann,[a] Aliki Kapazoglou,[c] Conrad W. Mullineaux,[e] Michael Hippler,[d] Jörg Nickelsen,[b] Peter J. Nixon,[c] and Olaf Kruse[a,1]

[a] Department of Biology/Molecular Cell Physiology, University of Bielefeld, 33501 Bielefeld, Germany
[b] Department of General and Molecular Botany, Ruhr-University Bochum, 44780 Bochum, Germany
[c] Division of Biology, Imperial College London, South Kensington Campus, London SW7 2AZ, United Kingdom
[d] Department of Biology, University of Pennsylvania, Philadelphia, Pennsylvania 19104
[e] Department of Biology, University College London, London WC1E 6BT, United Kingdom

Photosynthetic organisms respond to changes in ambient light by modulating the size and composition of their light-harvesting complexes, which in the case of the green alga *Chlamydomonas reinhardtii* consists of >15 members of a large extended family of chlorophyll binding subunits. How their expression is coordinated is unclear. Here, we describe the analysis of an insertion mutant, *state transitions mutant3* (*stm3*), which we show has increased levels of LHCBM subunits associated with the light-harvesting antenna of photosystem II. The mutated nuclear gene in *stm3* encodes the RNA binding protein NAB1 (for putative nucleic acid binding protein). In vitro and in vivo RNA binding and protein expression studies have confirmed that NAB1 differentially binds to *LHCBM* mRNA in a subpolysomal high molecular weight RNA–protein complex. Binding of NAB1 stabilizes *LHCBM* mRNA at the preinitiation level via sequestration and thereby represses translation. The specificity and affinity of binding are determined by an RNA sequence motif similar to that used by the *Xenopus laevis* translation repressor FRGY2, which is conserved to varying degrees in the *LHCBM* gene family. We conclude from our results that NAB1 plays an important role in controlling the expression of the light-harvesting antenna of photosystem II at the posttranscriptional level. The similarity of NAB1 and FRGY2 of *Xenopus* implies the existence of similar RNA-masking systems in animals and plants.

INTRODUCTION

In oxygenic photosynthesis, light energy is converted to chemical energy through the cooperation of two photosystems, photosystem I (PSI) and photosystem II (PSII). To compensate for changes in light intensity or spectral quality, plants and green algae have developed several short-term and long-term mechanisms to regulate the amount of light that is captured by each photosystem (Allen, 1992; Finazzi et al., 1999, 2001).

One long-term strategy that plants use to compensate for changes in light quality and quantity is to regulate the expression of the nucleus-encoded *LHC* gene family, which encodes the light-harvesting chlorophyll binding proteins (LHCII) of PSII (Escoubas et al., 1995; Durnford and Falkowski, 1997; Yang et al., 2001). For instance, the size of light antenna systems in

algae and plants increases under low irradiance to enhance the capture of photons by PSI and PSII, but it is reduced under high irradiances to prevent overexcitation of the photosystems and so avoid potential photooxidative damage (Anderson and Kay, 1995).

Regulation of LHCII expression is known to occur at many levels, including transcription initiation (Maxwell et al., 1995; Millar et al., 1995) and posttranscriptionally (Flachmann and Kühlbrandt, 1995; Lindahl et al., 1995; Durnford et al., 2003). As yet, little is known about these processes at the molecular level, especially translational control.

The LHCII proteins in the green alga *Chlamydomonas reinhardtii* are homologous with those found in higher plants (Teramoto et al., 2002). EST sequence analyses have revealed the existence of nine expressed LHCII isoforms (denoted LHCBM1 to LHCBM6, LHCBM8, LHCBM9, and LHCBM11 [Elrad and Grossman, 2004]), of which eight have now been identified at the protein level (Stauber et al., 2003). Although the LHCII proteins are structurally very similar, it is likely that individual gene products might have specific functions (Elrad et al., 2002).

Recently, we (Kruse et al., 1999) and others (Fleischmann et al., 1999; Depege et al., 2003) have established rapid chlorophyll fluorescence-based plate assays to screen for mutants impaired in nonphotochemical and photochemical fluorescence

quenching events, which include LHC state transitions (Bonaventura and Myers, 1969; Murata, 1969) and LHCII antenna size regulation. Here, we present the identification and characterization of the nuclear insertion mutant *state transitions mutant3* (*stm3*) from *C. reinhardtii*, which was identified using such a screen. Our analyses of this mutant led to the identification of an RNA binding protein that regulates the expression of a specific set of LHCII subunits at the posttranscriptional level and have provided new insights into how *C. reinhardtii* is able to fine-tune the expression of its light-harvesting antenna.

RESULTS

Light Harvesting Is Perturbed in *stm3*

To identify nuclear genes involved in regulating light harvesting within *C. reinhardtii*, we screened a library of mutants generated after the random insertion of plasmid *pSP124S*, which contains the *BLE* gene conferring phleomycin resistance (Stevens et al., 1996; Lumbreras et al., 1998), into the nuclear genome. A plate-based fluorescence video-imaging screen, which involves the recording of chlorophyll fluorescence from individual colonies before and after changing the relative excitation of PSI and PSII, was used to identify mutants affected in redistributing excitation energy between PSI and PSII (Kruse et al., 1999; Schönfeld et al., 2004). One such mutant, *stm3*, was subsequently confirmed to emit an unusually high level of chlorophyll fluorescence from the light-harvesting complexes (LHCII) associated with PSII (Figure 1A), despite the fact that PSII in *stm3* was as active as in the wild type, as assessed by chlorophyll fluorescence parameters (maximum photochemical efficiency of PSII in the dark-adapted state [F_v/F_m] = 0.79 in the wild type and 0.78 in *stm3*).

stm3 Contains a Single-Copy Insert and Its Phenotype Cosegregates with the BLE Cassette

DNA gel blot analysis confirmed that *stm3* contained a single copy of the *BLE* gene inserted in the genome (Figure 1B). To test whether the *BLE* marker was linked with the *stm3* phenotype, genetic crosses were performed between the wild type and *stm3* and the progeny scored for phleomycin resistance and the inability to show normal fluorescence characteristics, as assessed by video imaging. All 53 examined phleomycin-sensitive progeny exhibited a wild-type fluorescence phenotype, whereas progeny showing phleomycin resistance also showed a high-fluorescence phenotype (data not shown). These data suggested that the high-fluorescence phenotype of *stm3* was induced by the mutagenic event of plasmid DNA insertion.
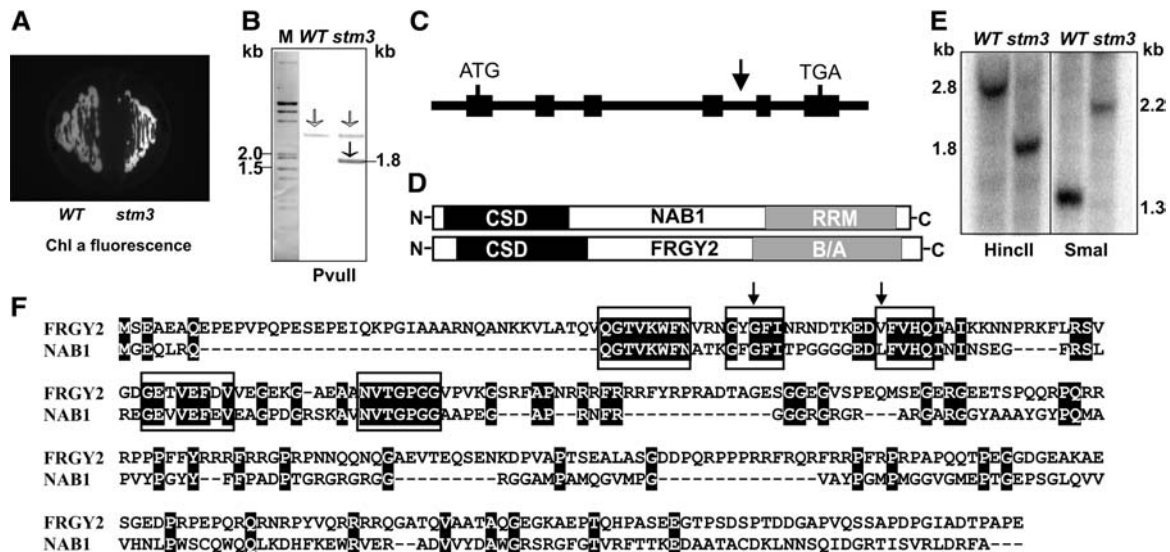
Figure 1. Identification of *stm3* by Fluorescence Spectroscopy and of the Nucleus-Encoded *NAB1* Gene in *C. reinhardtii*.

(A) PSII chlorophyll *a* fluorescence snapshot (55 μmol·m^{-2}·s^{-1}, 620 nm of actinic light) of wild-type and *stm3* colonies on Tris-acetate-phosphate (TAP) agar plates in a fluorescence video imager. Colonies were preilluminated for 20 min with 480 nm of blue light to fully gain state 2 conditions.

(B) DNA gel blot hybridizations with wild-type and *stm3* genomic DNA. Hybridizations were performed with a *pSP124S*-specific probe. Gray arrows indicate unspecific hybridization, and the black arrow indicates specific hybridization. M, marker.

(C) Model of the *NAB1* gene. DNA sequences were identified in the *stm3* genome by LMS-PCR (Strauss et al., 2001) and subsequent sequence analysis. Black boxes represent exons, and the arrow marks the plasmid *pSP124S* insertion site.

(D) Model of the NAB1 protein with an N-terminal CSD and a C-terminal RRM, and comparison with the *Xenopus* protein FRGY2. B/A, basic/aromatic region.

(E) DNA gel blot hybridizations with wild-type and *stm3* genomic DNA. Hybridizations were performed with a radioactively labeled 738-bp *NAB1*-specific probe.

(F) Amino acid sequence of the CSD of NAB1, and alignment with the *Xenopus* protein FRGY2. Boxes represent β-helix structures, and arrows represent functionally important Phe residues.

The Gene Disrupted in *stm3* Encodes a Putative Cytosolic RNA Binding Protein

Ligation-mediated suppression (LMS)-PCR (Strauss et al., 2001) was performed to analyze the plasmid insertion site and to clone the DNA flanking the *BLE* cassette in *stm3*. A plasmid fragment of ~2500 nucleotides, including the intact coding region of the *BLE* gene, was inserted into a putative open reading frame of the *stm3* genome. A total of 1900 nucleotides flanking the inserted vector were sequenced. Subsequent sequence analysis led to the identification of a nuclear gene with six exons and five introns (Figure 1C) encoding a putative 26.54-kD protein with two predicted nucleic acid binding domains: a cold-shock domain (CSD) at the N terminus and an RNA recognition motif (RRM) at the C terminus (Figure 1D). The gene and corresponding protein were designated NAB1 (for putative nucleic acid binding protein) and submitted to the databases. DNA gel blot analysis confirmed that the *NAB1* gene was disrupted in *stm3* (Figure 1E).

CSDs were originally identified in connection with cold-shock phenotypes (Jones et al., 1987). However, it is now established that this motif generally reflects a nucleic acid binding domain (Graumann and Marahiel, 1998). Detailed analysis of the *Chlamydomonas* genome databases suggests that NAB1 is the only protein that contains this CSD motif.

Overall, there were sequence similarities between NAB1 and several RRM domain–carrying Gly-rich proteins with different nucleotide binding functions, including GBP1, which is reported to bind single-stranded G-strand telomere DNA in *C. reinhardtii* (Petracek et al., 1994).

Another protein with high N-terminal sequence similarity to NAB1 is FRGY2 from *Xenopus laevis*. FRGY2 contains a N-terminal CSD motif (65% identity to NAB1 in the 68–amino acid domain) and, like NAB1, a second RNA binding domain at the C terminus (Matsumoto et al., 1996) (Figures 1D and 1F). Furthermore, analysis of NAB1 predicts structural similarities to FRGY2, including the presence of five β-helix structures (framed in Figure 1F) and functionally important Phe residues (arrows in Figure 1F) in the C-terminal RNA binding domain. FRGY2 is reported to mask maternal mRNAs in *Xenopus* oocytes and to control mRNA expression by repressing translation (Matsumoto et al., 1996; Manival et al., 2001). Initial RNA–protein binding via the CSD is followed by unspecific binding, coordinated by the second C-terminal RNA binding domain (Matsumoto et al., 1996).

RNA gel blot analysis confirmed the disruption of *NAB1* gene transcription (Figure 2A). To confirm that this disruption caused the phenotype in *stm3*, the mutant was transformed with a plasmid-borne intact wild-type copy of *NAB1*. A cotransformation approach using this *pNAB1* vector in combination with a second vector containing the *CRY1* gene conferring emetine resistance as a dominant selectable marker (Nelson et al., 1994) was applied. Of ~150 emetine-resistant colonies assessed, 4 were found to contain the *NAB1* gene.

Detailed analysis of one of them, designated *nc1*, showed that an intact *NAB1* gene had been incorporated into the genome (Figure 2B) and was expressed to wild-type levels, as judged by RT-PCR (Figure 2C) and immunoblot analysis (Figure 2F). Fluorescence video imaging confirmed that, in contrast with *stm3*,
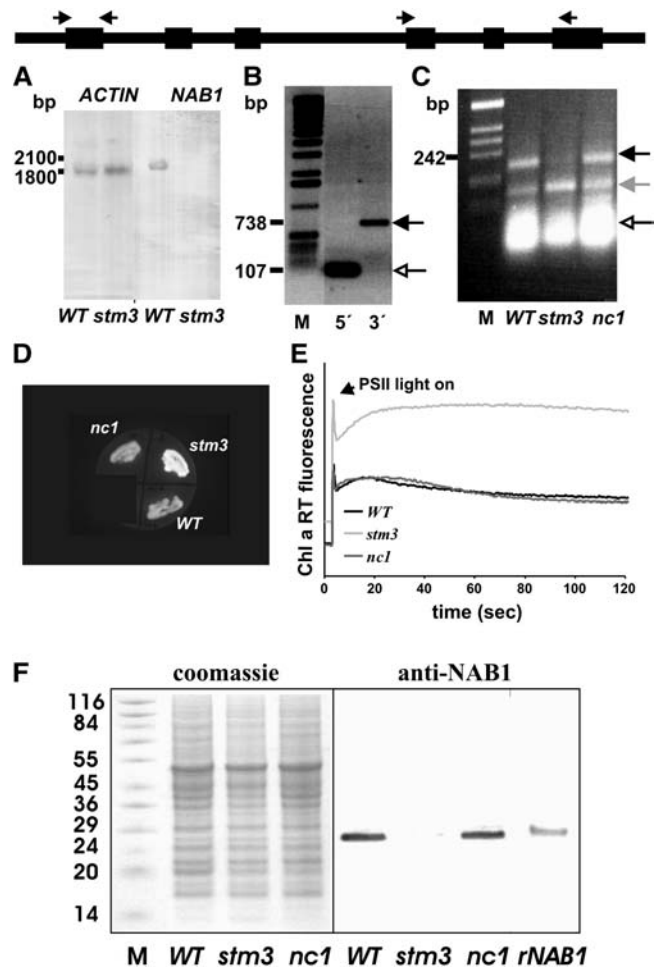
Figure 2. Evidence for the Disruption of *NAB1* Transcription in *stm3*, and Identification of the *NAB1* Complemented Strain *nc1* with a Reversed *stm3* Phenotype.

(A) RNA gel blot hybridizations with wild-type and *stm3* mRNA. Hybridizations were performed with a *NAB1*-specific probe.
(B) DNA analysis of the isolated strain *nc1* by PCR with primers amplifying either the 5′ (open arrow) or the 3′ (black arrow) region of the *NAB1* gene.
(C) RT-PCR analysis to detect *NAB1* expression using the same primers as in **(A)** amplifying the 3′ region. The black arrow marks specific *NAB1* amplification, the gray arrow marks unspecific amplification, and the open arrow marks degraded RNA. Arrows on the *NAB1* gene model mark primer positions used in **(A)** and **(B)**.
(D) Fluorescence video image taken from wild-type, *stm3*, and *nc1* colonies on TAP agar plates preincubated with PSII light to gain maximal state 2.
(E) Room-temperature (RT) fluorescence induction curves (Kautsky curves) of the wild type, *stm3*, and *nc1* over a period of 2 min. Dark-precultivated colonies were illuminated with 55 μmol·m^{-2}·s^{-1} actinic light on TAP agar plates, and fluorescence was recorded in a fluorescence video imager.
(F) Coomassie blue–stained SDS-PAGE gel and immunoblot with anti-NAB1. Wild-type, *stm3*, and *nc1* soluble proteins were derived from cell cultures. rNAB1, purified recombinant NAB1 protein.

nc1 performed normal state 2 activities in actinic light (Figure 2D) and showed wild-type levels of chlorophyll fluorescence, as judged by induction kinetics (the so-called Kautsky curve; Figure 2E). From these data and the fact that we could not detect any spontaneous reversion of *stm3* when vector *pNAB1* was omitted from the transformation experiment, we conclude that the disruption of *NAB1* is solely responsible for these defects in light harvesting.

Highly specific antibodies raised against recombinant NAB1 protein were used in immunoblotting experiments (Figure 2F) to confirm the expression of NAB1 (predicted size of 26.5 kD) in both the wild type and the complemented strain *nc1* but not in *stm3*. Immunogold labeling experiments (Figure 3) further indicated that NAB1 (visible in immunogold staining as black dots) was found in the cytosol (see zoomed sections b, c, and d) but not in the nucleus (section a), the mitochondria, or the chloroplast (section e). This result is consistent with the in silico analysis of the primary structure of NAB1, which suggested the absence of any N-terminal targeting sequence. Additionally, the location of NAB1 in the cytosol indicates that it is not involved in the binding of DNA, as described for a number of CSD proteins (Graumann and Marahiel, 1996).

stm3 Cells Contain Highly Stacked Thylakoid Membranes and More Chlorophyll per Cell and Are Sensitive to High Light

A striking feature of *stm3* was a dark-green phenotype caused by an ~50% greater total chlorophyll content per cell than in the wild type and *nc1* cultures grown in standard white light (Figure 4A). The higher chlorophyll content in *stm3* was accompanied by

a decrease in the chlorophyll *a/b* ratio from 2.45 and 2.51 (wild type and *nc1*, respectively) to 2.21 (*stm3*). Both results were clear indications of an increased LHC antenna system in the mutant.

Because the size and structure of light-harvesting antennae have been shown to influence the formation of granal stacks in chloroplasts (Allen and Forsberg, 2001; Yang et al., 2001), electron microscopy was performed to assess whether the thylakoid membrane structure was altered in *stm3*. Images were taken from wild-type, *nc1*, and *stm3* cells after cultivation to a log growth phase. The obtained images revealed remarkable differences in the arrangement of thylakoid membranes between the wild type, *nc1*, and mutant *stm3*, with the latter containing many more highly stacked granal regions (Figure 4A). This is in contrast with wild-type and *nc1* cells, in which thylakoid membranes were generally loosely arranged with more free-floating stroma lamellae interrupted by a few pseudograna structures (Figure 4A). *stm3* also contained more starch, which is an indication of physiological stress (Grossman, 2000).

Growth experiments under moderate high light (400 μmol·m^{-2}·s^{-1}) identified *stm3* as a light-sensitive strain (Figure 4B). A 43% reduction in growth rate of *stm3* cultures within 24 h of high-light incubation was accompanied by an 81% increase in cellular chlorophyll content, suggesting that an uncontrolled increase of the PSII–LHC antenna system in *stm3* caused photoinhibitory effects.

Inefficient energy transduction from LHC proteins to chlorophyll P_{680} attributable to a bigger antenna system would also explain the high-fluorescence phenotype of *stm3* and the observed decrease in ΦPSII quantum yields (0.55 in the wild type compared with 0.42 in *stm3*).
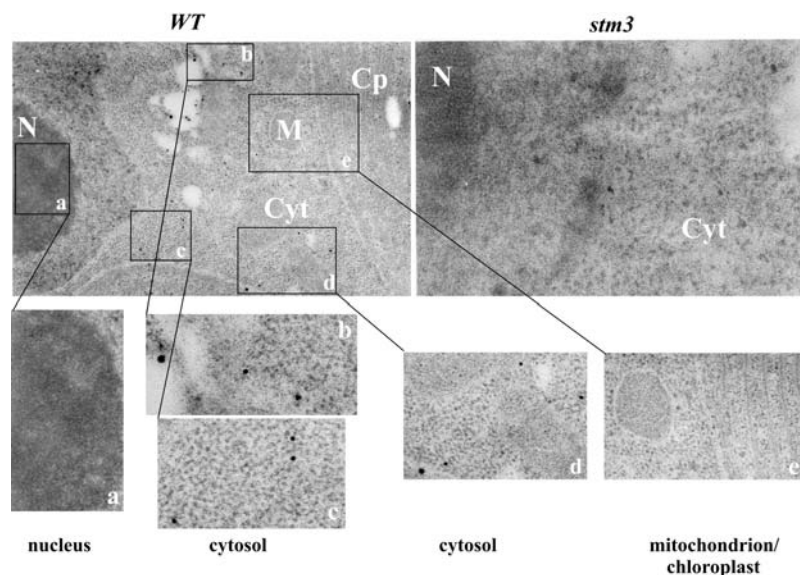
Figure 3. Localization of NAB1 in the Cytosol by Immunogold Labeling.

Electron micrographs of wild-type and *stm3* cell sections showing anti-NAB1 immunogold-labeled NAB1 proteins as black dots located in the cytosol of the wild type (zoomed sections b, c, and d) but not in the nucleus (zoomed section a), mitochondria, or chloroplast (zoomed section e). Cp, chloroplast; Cyt, cytosol; M, mitochondrion; N, nucleus.
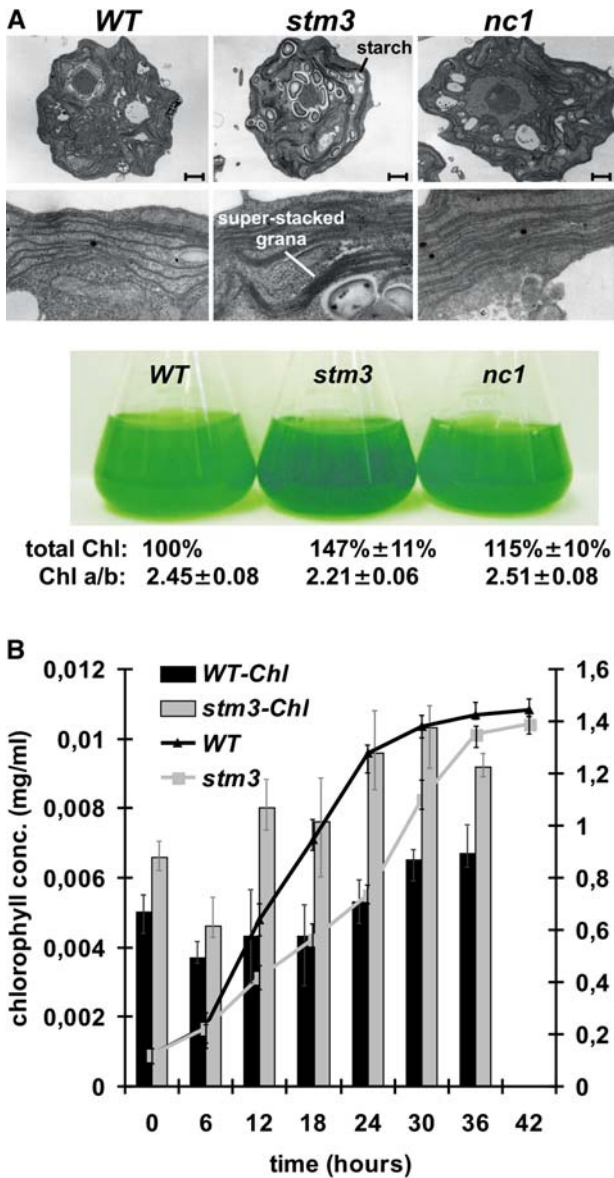
Figure 4. Characteristic Phenotypes of *stm3*.

(A) Electron micrographs of wild-type, *stm3*, and *nc1* cell sections ($\times13,000$ and $\times50,000$) showing super-stacked thylakoid membranes and higher starch incorporation in *stm3* cells compared with wild-type and *nc1* cells. Bars $= 1$ μm. At bottom is an image of the dark-green phenotype of *stm3* after growth in TAP medium and the corresponding chlorophyll (Chl) values. All cultures were set up to equal cell densities ($OD_{750} = 0.7$); cells were counted in a cell counter as a control.

(B) Growth rates and cellular chlorophyll concentrations during cultivation of wild-type and *stm3* cell cultures in 400 μmol·m^{-2}·s^{-1} moderate high light. Standard errors given for cell density and chlorophyll values are based on 10 independent measurements.

Loss of NAB1 Results in an Increase in Levels of LHCII Proteins in *stm3*

The high-chlorophyll fluorescence phenotype, the increase in total chlorophyll per cell, the decrease in the ratio of chlorophyll *a* to *b* in *stm3* compared with the wild type, the drastic changes in the chloroplast ultrastructure, and the sensitivity to moderate high light suggested that the disruption of *NAB1* caused an increase in the size, or perhaps a change in the composition, of the LHCII antenna system.

To test this, immunoblotting experiments were performed using antibodies raised against higher plant LHCII proteins. The results showed that the levels of LHCII proteins per cell had increased in *stm3* compared with the wild type (Figure 5A). Gel extraction of the two dominant immunoreactive bands followed by matrix-assisted laser desorption/ionization time-of-flight (MALDI-TOF) analysis suggested that these two bands consisted of LHCBM2/8 (lower band) and LHCBM4/6 (upper band) proteins.

To investigate this further, the LHCII proteins of the wild type and mutant were separated by two-dimensional gel electrophoresis. Immunoblotting was performed with antibodies raised specifically against the nearly identical N termini of LHCBM4 and LHCBM6 (Hippler et al., 2001). In agreement with previous work
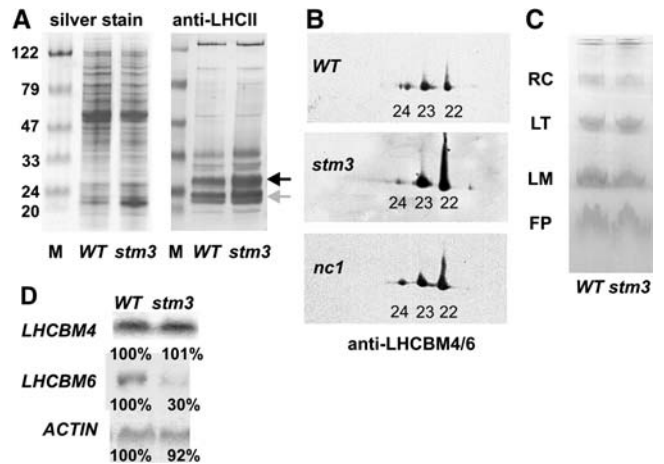
Figure 5. Effect of *NAB1* Deletion on LHC Antenna Protein Expression.

(A) One-dimensional electrophoresis of wild-type and *stm3* cell extracts based on equal cell density (OD_{750}, controlled by silver staining) and immunoblotting with anti-LHCII. The black arrow marks the LHCBM4/6 protein band, and the gray arrow marks the LHCBM2/8 protein band, as identified by MALDI-TOF analysis.

(B) Immunoblots probed with anti-LHCBM4/6 peptide antibodies (Hippler et al., 2001) after protein separation with pH-dependent two-dimensional gel electrophoresis of wild-type, *stm3*, and *nc1* thylakoid membranes. Spots 22, 23, and 24 were assigned according to Hippler et al. (2001).

(C) Native gel electrophoresis of wild-type and *stm3* thylakoid membranes based on equal chlorophyll concentrations. FP, free pigments; LM, LHCII monomers; LT, LHCII trimers; RC, reaction centers.

(D) RNA gel blot analysis of *LHCBM4* and *LHCBM6* mRNA concentrations in standard light-cultivated wild-type and *stm3* cultures. Gene-specific probes were derived from the 3′ UTR, and actin was used as a control for equal loading.

(Stauber et al., 2003), the antibodies recognized three spots in the wild type, *stm3*, and *nc1* (spots 22, 23, and 24) indicating that the increase of LHCBM4/6 protein levels in *stm3* was not accompanied by the appearance of further modified LHCBM4/6-type proteins in the mutant (Figure 5B). Interestingly, however, the levels of spots 22 and 23 relative to spot 24 increased drastically in *stm3* compared with the wild type and the complemented strain *nc1* (Figure 5B).

Detailed analysis of all three spots by tandem mass spectrometry has so far revealed only one difference between spots 22/23 and spot 24: all three spots contain LHCBM4 peptide fragments, but LHCBM6-specific peptide fragments were identified only in spots 22 and 23, not in spot 24 (Stauber et al., 2003). These data suggested that the deletion of NAB1 in *stm3* caused a change in the LHCBM4/LHCBM6 protein expression ratio. Analysis of detergent-solubilized thylakoids by native gel electrophoresis confirmed that the altered LHCII composition in *stm3* did not prevent the formation of trimeric LHCII complexes (Figure 5C).

To assess whether the increased abundance of LHCII proteins found in *stm3* was attributable to an increased pool for *LHCBM* transcripts, RNA gel blot experiments were performed with probes specific for *LHCBM4* and *LHCBM6*. Interestingly, these blots revealed that *LHCBM6* transcript levels were reduced by nearly 70% in standard light-cultivated *stm3* cells compared with wild-type cells, whereas *LHCBM4* transcript levels showed almost no differences between the mutant and the wild type (Figure 5D).

Recombinant NAB1 Binds *LHCBM4* and *LHCBM6* mRNA via Its N-Terminal CSD Motif in Vitro with Different Affinities

The results obtained so far suggested a model in which NAB1 might act bifunctionally at a posttranscriptional level to stabilize transcripts and to repress the translation of *LHCBM* mRNAs. In the absence of NAB1, expression of these genes would be upregulated. Based on the similarity to the CSD of FRGY2 from *Xenopus*, in silico searches were performed to identify potential NAB1 binding sites within *LHCBM* mRNAs. Indeed, the mRNA consensus sequence motif (CSDCS), which is specifically recognized by the CSD of FRGY2 (GCCANACCAC/UCGC [Manival et al., 2001]), could be found with different degrees of sequence conservation in the coding regions of *LHCBM1*, *-2*, *-3*, *-4*, *-5*, *-6*, *-8*, and *-9* cDNAs (Figure 6A). It should be noted that *LHCBM7* and *LHCBM10* were excluded from the original list of *C. reinhardtii LHCBM* genes (Elrad et al., 2002) because, in agreement with recent results (Elrad and Grossman, 2004), we could not identify their products as independent isoforms, either in the nuclear genome or during intensive tandem mass spectrometry analyses of LHCBM proteins (Stauber et al., 2003).

To test the putative RNA binding activity of NAB1, UV cross-linking assays were performed in vitro. As shown in Figure 6B, recombinant NAB1 was able to bind to a radiolabeled RNA probe comprising the *LHCBM6* CSDCS. In addition, competition experiments with various unlabeled RNA probes containing either the CSDCS region or sequences from the 5′ or 3′ untranslated region (UTR) of the *LHCBM6* mRNA revealed that NAB1 bound with very high affinity to CSDCS and only weakly to the 5′ or 3′ UTR. By contrast, an unrelated AU-rich RNA probe from the chloroplast *psbD* gene was not recognized at all by NAB1 (Figure 6B).

To further elucidate the role of the CSD recognition motif for specific *LHCBM6* RNA binding, we changed a single nucleotide (A to T at position 4 of the recognition motif) in the *LHCBM6* RNA sequence. This mutation resulted in a new sequence that now matched exactly with the CSDCS recognition motif of *LHCBM4* mRNA. As a result of this single nucleotide exchange, the binding affinity of NAB1 decreased drastically (Figure 6B). This finding clearly showed that the putative CSD recognition motif CSDCS is functionally involved in NAB1 binding and suggested that the CSD of NAB1 plays an important role similar to FRGY2. Furthermore, the reduced binding of NAB1 to the *LHCBM4*-type recognition site motif showed that recombinant NAB1 discriminates between different *LHCBM* RNAs in vitro, suggesting that it might have a similar function in vivo.

By analogy with the function of FRGY2, the sequence specificity of NAB1 binding should be mediated via its CSD. To test this hypothesis, in vitro binding studies were performed with a 10-kD N-terminal NAB1 fragment that contains the complete CSD motif but lacks the C-terminal RRM domain (Figure 6C). In agreement with our hypothesis, the 10-kD CSD fragment of NAB1 showed a high and specific binding affinity to the CSDCS recognition motif of *LHCBM6* RNA, similar to the results obtained with native NAB1 protein. Again, the binding affinity to the *LHCBM4*-type recognition site was reduced drastically (Figure 6C).

We conclude from the in vitro studies that NAB1 is indeed an RNA binding protein and that it binds via its CSD with different affinities to *LHCBM* mRNAs.

NAB1 Binds *LHCBM6* RNA in Nontranslated Messenger Ribonucleoprotein Complexes

From our in vitro studies, NAB1 would represent a protein that binds and sequestrates *LHCBM* mRNAs at a subpolysomal level, thus acting to fine-tune the expression of LHCBM6 proteins in *C. reinhardtii*. To investigate this hypothesis, cytosolic mRNA was isolated from wild-type and *stm3* cells in the presence of cycloheximide, separated into subpolysomal nontranslated messenger ribonucleoproteins (mRNPs) and monosomal and translated polysomal complexes by sucrose density gradient centrifugation (15 to 45% sucrose) (Barkan, 1988; Shama and Meyuhas, 1996; Yohn et al., 1996), and further analyzed.

Combined *LHCBM6* RNA slot blot (Figure 6D, middle panel) and anti-NAB1 immunoblot (Figure 6D, bottom panel) studies were performed in all 18 separated fractions derived from the sucrose gradients of the wild type and *stm3*.

From the appearance of 18S RNA (representing the 40S subunit) and 25S rRNA (part of the 60S subunit) (Marco and Rochaix, 1980) in the separated fractions of the wild type (Figure 6D, top panel), we concluded that fractions 1 to 4 contain only nontranslated RNA in subpolysomal preinitiation complexes (mRNPs ± 40S subunits). By contrast, fractions 5 to 18 contain ribosomal complexes including 40S and 60S subunits (monosomes) and, from approximately fraction 8 onward, polysomes (Shama and Meyuhas, 1996). Protein and RNA gel blot studies with wild-type samples revealed that the vast majority of NAB1 cofractionates in fractions 2, 3, and 4 with preinitiation (mRNP − 40S) complexes (molecular mass of 400 to 900 kD). Most interestingly, in the wild type these fractions contained 40%
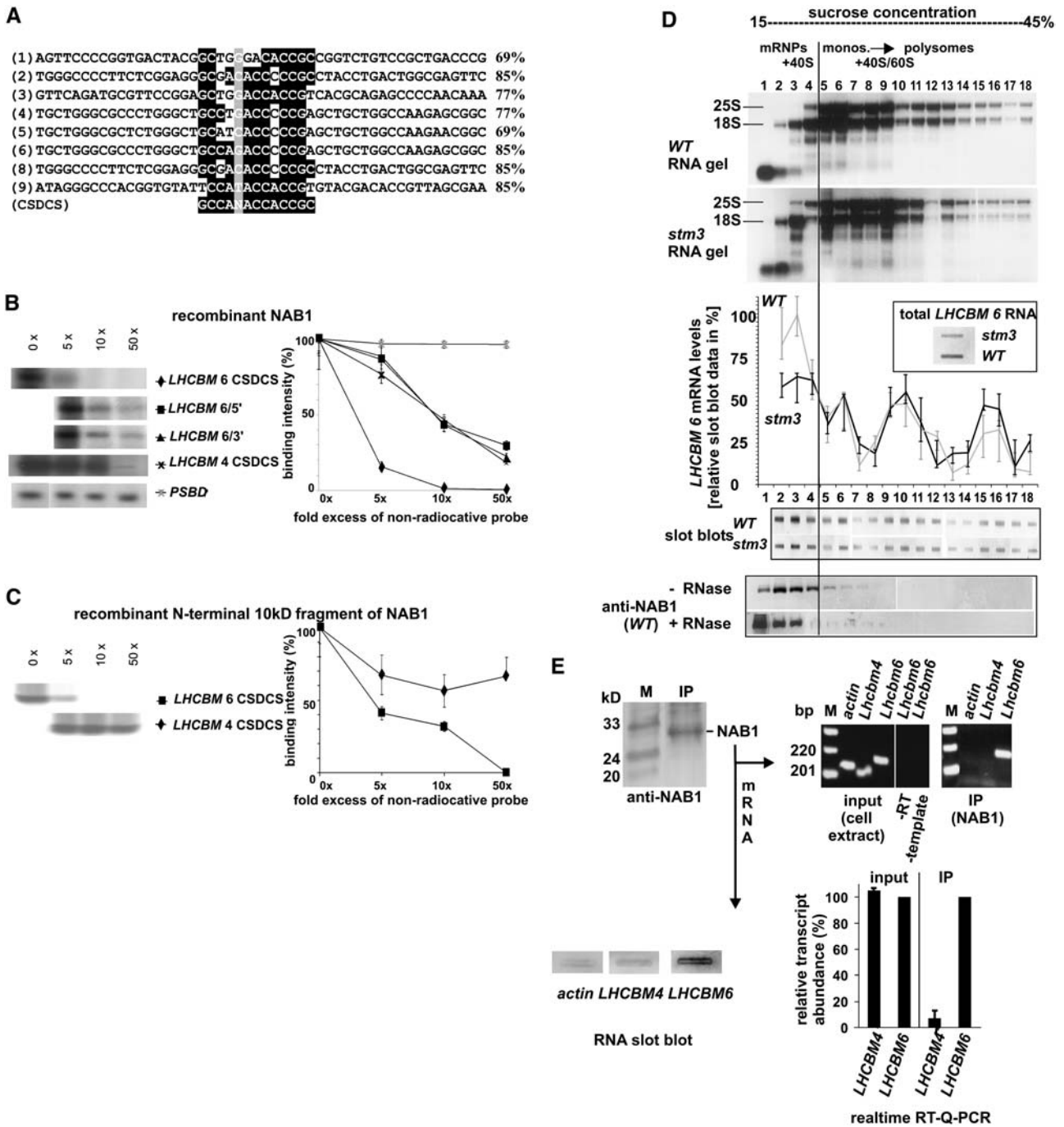
Figure 6. Function of NAB1 as an RNA Binding Translation Regulator.

(A) Sequence alignment of *LHCBM1* to *LHCBM9* [(1) to (9)] cDNAs from *C. reinhardtii* with the consensus motif (CSDCS) recognized by FRGY2 from *Xenopus*. Identical positions are indicated by a black background, and sequence identity levels are given at right.

(B) In vitro RNA binding competition studies. Autoradiogram after UV cross-linking of recombinant NAB1 protein, radiolabeled *LHCBM6*-CSDCS RNA probe, and a 5-, 10-, and 50-fold molar excess of the indicated nonlabeled competitor RNAs. The exposure time was identical for all lanes. Competition with *PSBD* 5′ UTR RNA was performed independently. Quantification of RNA binding intensities in relation to the NAB1 signal without competitor (0× value) from one representative experiment was estimated by signal densitometry and plotted as a diagram.

(C) In vitro RNA binding studies. Autoradiogram after UV cross-linking of recombinant N-terminal 83–amino acid NAB1 peptide fragment (carrying the complete CSD) and radiolabeled *LHCBM6*-CSDCS RNA probe (for details, see **[B]**). Indicated competitor RNAs were added in 5-, 10-, and 50-fold molar excess to the reactions.

higher levels of *LHCBM6* RNA compared with *stm3* (Figure 6D). This is not the case with actively translating heavy polysomes; both strains contained comparable levels of *LHCBM6* RNA.

Partial digestion of RNA–protein complexes by RNase treatment of the wild-type sample before sucrose density fractionation resulted in the appearance of vast amounts of unbound NAB1 protein on top of the gradient (fraction 1), whereas NAB1–RNA high molecular weight complexes fully disappeared in fractions 4, 5, and 6.

To confirm that NAB1 does indeed bind to *LHCBM6* RNA in vivo, we isolated native NAB1 protein by immunoprecipitation from soluble wild-type cell fractions using polyclonal NAB1 antibodies. Successful purification of native NAB1 was confirmed by immunoblotting (Figure 6E). Subsequent isolation of RNA from the purified NAB1 protein followed by slot-blot analysis and by quantitative real-time RT-PCR analysis confirmed highly abundant binding of *LHCBM6* mRNA [cycle threshold, C(T), value of 16.9] to NAB1, whereas only very low concentrations of *LHCBM4* mRNA were detected [C(T) value of 28.1] (Figure 6E).

In conclusion, these data show that NAB1 proteins are functionally located in subpolysomal nontranslated high molecular weight RNA–protein complexes of the cytosol, where they preferentially bind and sequestrate *LHCBM6* mRNA and, to a very low level, *LHCBM4* mRNA. Such a posttranscriptional control mechanism would enable the cell to acclimate to environmental changes by a fast expression of light-harvesting antenna proteins through the permanent pool of stored *LHCBM6* mRNA.

LHCBM Protein Expression Studies Confirm the Important Role of NAB1 in Light-Induced Posttranscriptional Control of LHCII Gene Expression

To elucidate the functional role of NAB1–RNA binding on the light-harvesting protein expression level, we used a hemagglutinin (HA) tag–*LHCBM* gene construct (Imbault et al., 1988; Stauber et al., 2003) and introduced an A-to-T exchange at position 4 of the CSDCS recognition motif by site-directed mutagenesis to get hold of two HA-tagged LHCBM proteins, one with a *LHCBM6*-type CSDCS recognition motif (later described as HA-LHCBM6) and one with a *LHCBM4*-type recognition motif (later described as HA-LHCBM4). Both genes were cloned into vector *pGenD* (Fischer and Rochaix, 2001) for transcription under the control of the high-expression psaD promoter.

This cloning strategy had two advantages. First, the use of an alternative promoter inactivated redox-regulated promoter-induced *LHCBM* transcription control for these genes (Teramoto et al., 2002). Second, the HA tag enabled us to estimate the level of differential LHCBM protein expression by quantitative immunoblot analysis. Both constructs were transformed into the wild type and *stm3* and subsequently used for in vivo expression studies under different light conditions.

Immunoblot analysis of cell samples from standard grown cultures and cultures treated with moderate high light (180 μmol·m^{-2}·s^{-1}) was performed using anti-HA antibodies. With standard *LHCBM* transcription control perturbed by the use of an alternative promoter, cultivation of wild-type HA-LHCBM4 clones for 24 h under moderate high light caused no decrease of LHCBM4 protein expression levels, indicating that neither transcriptional nor posttranscriptional downregulation occurred (Figure 7). By contrast, moderate high light–cultivated wild-type HA-LHCBM6 clones showed a dramatic 72% decrease of HA-LHCBM6 protein levels, indicating that the light treatment initiated control mechanisms (Figures 7A to 7D). It should be noted that the appearance of two protein bands reflect the existence of two processed forms of HA-LHCBM6 (Stauber et al., 2003).

Real-time RT-PCR analysis of HA-*LHCBM6* mRNA revealed that, in contrast with the decrease in protein concentration, *LHCBM6* transcript levels were almost unchanged in the selected HA-LHCBM6 wild-type and *stm3* strains under different light regimes (Figure 7E). This finding clearly demonstrated that the decrease in HA-LHCBM6 protein level is a posttranscriptional effect and not caused by the light-induced repression of *HA-LHCBM6* gene transcription.

Our results confirmed earlier observations in *C. reinhardtii* that long-term light treatment does not yield an overall decrease of *LHCBM* transcript levels, whereas protein expression levels decrease drastically (Durnford et al., 2003), which highlighted the existence and relevance of posttranscriptional control of light-harvesting proteins.

We concluded from the HA-LHCBM expression data that, in agreement with our other results, LHCBM6 expression is much more affected by light-induced posttranscriptional effects than LHCBM4.

Furthermore, our results clearly confirmed the important regulatory role of NAB1: *stm3* HA-LHCBM6 clones reacted far more insensitively to the light treatment compared with their

---

Figure 6. (continued).

(D) Analysis of high molecular weight subpolysomal and polysomal RNA–protein fractions derived from wild-type and *stm3* cell extracts after 15 to 45% sucrose gradient centrifugation. Isolated RNA from each fraction separated by gel electrophoresis (top panel), and *LHCBM6* mRNA levels determined by RNA slot blotting (middle panel; standard errors are based on five independent measurements). Identification of fractions containing NAB1 proteins by anti-NAB1 immunoblotting of nontreated samples (− RNase) and samples pretreated with RNase before centrifugation and separation (+ RNase) (bottom panel).

(E) In vivo mRNA binding studies. Anti-NAB1 immunoblot showing purification of immunoprecipitated (IP) native NAB1 from cell extracts, and analysis of bound mRNA by slot-blot analysis and real-time RT-quantitative (Q)-PCR using probes and primers specific for *LHCBM6*, *LHCBM4*, and *ACTIN*. The agarose gel shows transcript abundance after 25 cycles. mRNAs from input cell extracts were used as a positive control. *ACTIN*, *LHCBM4*, and *LHCBM6* transcripts became detectable after 14 to 16 cycles. Samples without reverse transcriptase (−RT) or template were used as negative controls. *LHCBM6* transcripts in RT-Q-PCR studies, using immunoprecipitated NAB1-derived mRNA as a template, became detectable after 16 cycles, whereas *LHCBM4* and *ACTIN* transcripts did not appear before cycles 28 and 39, respectively. Rates for relative transcript abundance are calculated from five independent measurements as $2^{-[C(T)\ transcript\ -\ C(T)\ actin]}$, where C(T) = cycle values. The *LHCBM6* values were set to 100%.
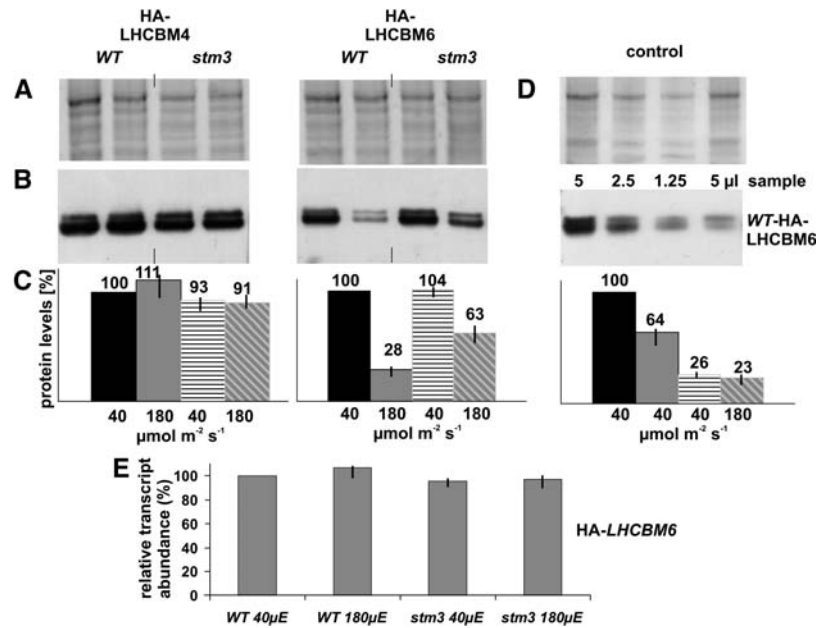
Figure 7. Wild-Type and *stm3* Protein Expression Studies of HA-Tagged LHCBM Proteins Carrying Either the *LHCBM4*-Type CSDCS Motif (HA-Tagged LHCBM4) or the *LHCBM6*-Type CSDCS Motif (HA-Tagged LHCBM6) under Different Light Regimes.

(A) Coomassie blue–stained SDS protein gels as controls for equal loading.

(B) Anti-HA tag immunoblots to detect protein levels of HA-tagged LHCBM4 and LHCBM6 in the wild type and *stm3* grown in standard light (40 μmol·m^{-2}·s^{-1}) or after treatment for 48 h with moderate high light (180 μmol·m^{-2}·s^{-1}).

(C) Quantification of LHCBM4/6 protein expression levels using GelScan 2.0.

(D) Quantification control experiment. Dilution series (5, 2.5, and 1.25 μL) of wild-type HA-LHCBM6 samples grown in standard light and compared with a 5-μL sample grown in moderate high light.

(E) Real-time RT-quantitative-PCR studies to evaluate *LHCBM6* mRNA levels derived from wild-type and *stm3* HA-LHCBM6 cell extracts.

Standard errors in **(C)** and **(E)** are based on three independent measurements.

wild-type HA-LHCBM6 counterparts and exhibited a decrease of 37% in LHCBM6 abundance (Figure 7C).

From these results, we could assign ~50% of the observed decrease in LHCBM6 protein level upon light treatment in the wild type to functional NAB1 binding with *LHCBM6* mRNA, whereas the other 50% decrease, which occurs in both strains, must be assigned to additional posttranscriptional effects, such as protein degradation (Lindahl et al., 1995).

In summary, our results have clearly identified with NAB1 a novel cytosolic RNA binding protein that functionally binds *LHCBM* RNA through a *LHCBM* CSDCS recognition motif. NAB1 forms high molecular weight nontranslated mRNP complexes in the cytosol in which *LHCBM6* RNA is sequestered and thereby prevented from translation in polysomes.

DISCUSSION

Mutant *stm3* Shows Aberrant Expression of the LHCII Antenna

The dark-green phenotype (Figure 4), the decrease in chlorophyll *a/b* ratio, the highly stacked grana, and the changes in LHCBM protein expression pattern (Figure 5) are clear indicators of an altered LHCII antenna system in *stm3*. Our data strongly suggest

that absence of NAB1 causes the increased expression of certain LHCBM proteins, thus leading to an overall increase in the size of the LHCII antenna. The similarity of the chlorophyll fluorescence parameter (F$_v$/F$_m$) in the wild type and *stm3* suggests that the additional antenna is still coupled to PSII reaction centers in *stm3*. If the additional antenna proteins were partially uncoupled, the initial (minimum) PSII fluorescence in the dark-adapted state (F$_0$) would be expected to increase, leading to an overall decrease in the F$_v$/F$_m$ ratio.

It should be noted that the observed phenotype of perturbed LHC state transitions in *stm3* is most likely an indirect effect of the super-stacked grana organization caused by an altered antenna structure attributable to the disruption of the LHCBM expression profile.

The similarity of NAB1 to FRGY2 of *Xenopus* implies the existence of similar RNA-masking systems in animals and *Chlamydomonas*.

Complementation experiments have clearly confirmed that the effects on the LHCII antenna of *stm3* are attributable to the inactivation of *NAB1*. NAB1 contains two RNA binding domains with a CSD motif at the N terminus and a RRM at the C terminus. The existence of two different RNA binding domains on one protein has been described previously (Graumann and Marahiel, 1998). However, we did not identify any other proteins with the

combination of CSD and RRM domains. Database searches have only identified 13 complete protein sequences with CSDs in plants (data not shown), five of them in *Arabidopsis thaliana* (AtGRP2, AtGRP2b, At2g17870, At4g36020, and At4g38680). Analysis of the *Chlamydomonas* genome indicates that NAB1 is the only protein in *C. reinhardtii* with a CSD. This result underlines the unique and special character of the RNA binding protein NAB1.

Temperature shock experiments (0 to 24 h at 4, 20, and 40°C; data not shown) did not reveal any obvious visual phenotypic difference between *stm3* and the wild type, which suggests that NAB1 is not essential for temperature acclimation.

Interestingly, there are many striking similarities between NAB1 and the *Xenopus* RNA binding protein FRGY2. FRGY2 contains a CSD responsible for initial protein–RNA binding and a second RNA binding domain at its C terminus for effective RNA binding (Matsumoto et al., 1996; Manival et al., 2001). As soon as the initial binding has occurred at the CSD, more FRGY2 proteins bind to the target RNA with their unspecific C-terminal binding domain, leading to a repression of RNA translation.

Detailed analysis of the protein–RNA interaction site has led to the identification of an RNA binding consensus domain, which is needed for a specific CSD binding in FRGY2 (Manival et al., 2001). Database searches revealed that a similar 13-nucleotide sequence is found in *LHCBM2*, *LHCBM6*, *LHCBM8*, and *LHCBM9* (85% identity). For the other *LHCBM* genes, the sequence is less conserved (69 to 77% identity).

NAB1 Is a Cytosolic Translation Repressor and Essential for RNA Stabilization and Sequestration

Immunogold localization studies have confirmed that NAB1 is indeed localized in the cytosol (Figure 3). This result excludes a bifunctional role for NAB1 as both an RNA and DNA binding protein. The analysis of nuclear protein localization by immuno-gold labeling is often affected by false-positive protein signals in the nucleus. In our case, however, the highly specific anti-NAB1 antibody showed no nuclear cross-reaction at all, which clearly demonstrated that NAB1 is not localized in the nucleus.

In vitro RNA binding studies with recombinant NAB1 protein, as well as with N-terminal CSD fragments of NAB1, have suggested that protein–RNA interaction is mediated by the specific binding of the CSD to a CSDCS RNA consensus domain in *LHCBM6* (Figures 6B and 6C). In vivo binding studies confirmed the role of NAB1 as a functional RNA binding protein that preferentially binds *LHCBM6* RNA (Figure 6E). The obtained drastic difference in NAB1–RNA binding capacity between *LHCBM4* and *LHCBM6* in conjunction with the clear differences in the abundance of LHCBM4 and LHCBM6 proteins in the wild type and *stm3* support a role for NAB1 in the differential expression of LHCBM subunits in *C. reinhardtii*. However, it should be noted that several other predicted mRNAs contain potential CSDCS-like binding domains, which makes it possible that the RNA binding activity of NAB1 is not limited to *LHCBM* mRNAs.

Immunoblot and RNA slot-blot analyses of subpolysomal and polysomal RNA fractions from sucrose gradients (Figure 6D), *LHCBM4/6* RNA gel blot analyses (Figure 5D), in vivo RNA binding studies by immunoprecipitation and real-time RT-PCR (Figure 6E), in vitro RNA binding studies (Figures 6B and 6C), and

protein expression studies with *LHCBM4/6* transcription control–insensitive clones of the wild type and *stm3* (Figure 7) support a model in which NAB1 functionally occurs in subribosomal high molecular weight protein–RNA complexes in which it binds to *LHCBM* mRNAs with different affinities, sequesters them, and represses translation. The clear difference in NAB1 binding affinity between *LHCBM4* and *LHCBM6* mRNA explains why in its absence in *stm3*, LHCBM6 expression is much more affected than LHCBM4 expression (Figure 5B).

This is further supported by the drastic differences obtained for LHCBM4 and LHCBM6 expression by moderate high-light treatment. HA tagging allowed quantitative estimation of protein levels by immunoblotting and revealed that *LHCBM4* RNA translation is not influenced by light, whereas *LHCBM6* RNA translation clearly is (Figure 7).

The observed reduced level of *LHCBM6* transcripts in *stm3* compared with the wild type (Figure 5D) could be explained by the absence of *LHCBM6* RNA sequestration in the mutant, leading to an increase of RNA instability and degradation, similar to the function described for FRGY2 (Matsumoto et al., 2003) and YB-1, another CSD protein involved in mRNA translation control (Evdokimova et al., 2001). From our studies, it is feasible to suggest the existence of similar RNA-masking systems in animals and *Chlamydomonas*. As with FRGY2 and YB-1, NAB1 contains two RNA binding domains, with one of them a CSD at the N terminus for specific RNA binding.

LHCII Antenna Size in *C. reinhardtii* Is Controlled at Many Levels

It is well established that the expression of LHCII proteins is regulated at the level of gene transcription (Shepherd et al., 1983; Escoubas et al., 1995; Maxwell et al., 1995; Teramoto et al., 2002). Under low-light conditions, *LHCBM* mRNA levels increase, whereas levels decrease under increasing light conditions (Elrad and Grossman, 2004). A specific role of the redox state of the plastoquinone pool as a sensor of the imbalances in photosynthetic electron transport has been proposed (Escoubas et al., 1995).

In addition, expression of some photosynthesis genes is also controlled at the translational level (Danon and Mayfield, 1994; Danon, 1997; Petracek et al., 1997; Drapier et al., 2002). This can be of particular importance for light-regulated chloroplast proteins that are encoded in the nucleus. In this case, a steady state pool of mRNA in the cytosol would enable the cell to respond faster to events in the chloroplast. However, the existence of ready-to-use mRNA requires a stress-dependent regulation system that operates at the posttranscriptional level. To date, there has only been indirect evidence to indicate the existence of posttranscriptional control of LHC protein expression (Flachmann and Kühlbrandt, 1995; Tang et al., 2003). However, recent results (Durnford et al., 2003) have revealed that posttranscriptional control becomes more important than redox-regulated transcription regulation under long-term stress conditions. The work described here on the identification of NAB1 gives new insights into how posttranscriptional control of light harvesting is achieved in *C. reinhardtii*. It complements the picture emerging through other recent work about eukaryotic gene expression and

shows that posttranscriptional control is an elaborate way in which the cell regulates and adjusts adequate protein synthesis (Moore, 2005).

METHODS

Strains and Culture Conditions

Liquid cultures of *Chlamydomonas reinhardtii* were grown in continuous white light (40 μmol·m^{-2}·s^{-1}). TAP and high-salt media were prepared as described (Harris, 1989), 1.5% Select Agar (Gibco BRL) was added to prepare solid plates, and 13 μM phleomycin (Sigma-Aldrich) or 100 μM emetine dihydrochloride (Sigma-Aldrich) was added for screening of *pSP124S* or *p613* transformant, respectively. TAP 1:10 N was prepared by reducing the amount of NH$_4$Cl to 1:10.

Mutant Construction and Genetic Analysis

Mutant *stm3* was generated in the background of *Chlamydomonas* strain CC849 (Duke University) by transformation with plasmid *pSP124S* (Stevens et al., 1996; Lumbreras et al., 1998) as described previously (Kindle, 1990) and grown on TAP medium containing phleomycin to test for resistance to the drug. Generation of gametes, matings, and zygote analysis were performed as described (Harris, 1989).

Isolation of Nucleic Acids, and Hybridizations

Manipulations of nucleic acids were performed according to standard methods (Sambrook et al., 1989). For DNA gel blot analysis, DNA of the wild type and *stm3* was restricted with *Pvu*II, *Hinc*II, or *Sma*I enzymes and probed with labeled PCR products synthesized with primer pairs 5′-ATGGCCAGGATGGCCAAGC-3′ and 5′-TTAGTCCTGCTCCTCGG-CCACG-3′ for *pSP124S* or 5′-CCATGCAGGGCGTGAT-3′ and 5′-GTC-CTCCTTGGTCGTGAAGC-3′ for *NAB1*.

LMS-PCR

Genomic DNA flanking the inserted vector in *stm3* was identified by LMS-PCR (Strauss et al., 2001). LMS adapters were ligated, and suppression PCR was performed with vector-specific primer and adapter-specific primer. The PCR product was used as a template in a second, nested LMS-PCR. The resulting DNA fragment of apparently 2 kb was gel-extracted, cloned into pGEM-T Easy vector (Promega), and sequenced.

Chlorophyll Fluorescence Measurements

Room-temperature fluorescence video imaging to detect mutants with perturbed state transitions was performed as described (Kruse et al., 1999). Kautsky fluorescence induction was recorded by illuminating dark-adapted cells for 2 min with 55 μmol·m^{-2}·s^{-1} red light (620 nm).

F_v/F_m was recorded from dark-adapted cells in saturating white light and calculated by $F_v/F_m = (F_m - F_0)/F_m$. ΦPSII was measured by illuminating dark-adapted cells with actinic light (620 nm, 55 μmol·m^{-2}·s^{-1}) and calculated by $(F'_m - F_t)/F'_m$ (Maxwell and Johnson, 2000), where F_t is steady state fluorescence yield.

Complementation Experiments

For complementation of *stm3*, the *CRY1* gene, conferring resistance to emetine (plasmid *p613*) (Nelson et al., 1994), was used as a dominant selectable marker together with plasmid *pNAB1* containing the complete nuclear *NAB1* gene cloned into pBluescript II SK− (Stratagene). *stm3* cells were transformed with 2 μg of each plasmid by the glass bead method (Kindle, 1990). Transformed cells were incubated in TAP 1:10 N for 4 d, resuspended in TAP medium for 8 h, and spread onto TAP$_{Emetine}$ plates. Colonies appeared after 12 d and were screened for the integration of *pNAB1* by PCR. RNA was isolated (RNeasy mini kit; Qiagen) from PCR-positive clones and reverse-transcribed (Genescript reverse transcriptase; Genecraft), and RT-PCR was performed with *NAB1*-specific primers.

Overexpression of NAB1 and Fragmentation

NAB1 cDNA was cloned into a pQE80L vector (Qiagen) and transformed into *Escherichia coli* strain M15. Overexpression and purification of the N-terminally 6× His-tagged NAB1 protein were performed according to the manufacturer's instructions (Qiagen). An N-terminal 83–amino acid peptide fragment of recombinant NAB1 was purified by nickel–nitrilotriacetic acid agarose column chromatography after thrombin digestion.

Cloning of HA-Tagged *LHCBM* Genes

An HA epitope–tagged form of the *LHCBM6* gene was cloned into the pGEM-T Easy vector (Promega) and modified by in vitro PCR mutagenesis (QuikChange; Stratagene) to replace adenine at position 730 by thymidine in *LHCBM6*, which resulted in a nucleotide sequence identical to the CSDCS recognition motif (Matsumoto et al., 1996) of *LHCBM4*. Genes were ligated into the *PSAD* promoter–containing expression vector *pGenD* (Fischer and Rochaix, 2001) and cotransformed using the *CRY1* marker gene as described above. Potential cotransformants were screened by immunoblotting using a HA-specific monoclonal antibody (Roche). For moderate high-light treatment, cells were illuminated with white light (180 μmol·m^{-2}·s^{-1}) for 22 h.

Gel Electrophoresis and Immunoblotting

Proteins were separated by SDS-gel electrophoresis and subsequently electroblotted onto nitrocellulose membranes (Amersham). Sample preparation for two-dimensional gel electrophoresis is described elsewhere (Hippler et al., 2001). Native green gels were prepared as described (Allen and Staehelin, 1991). His-tagged NAB1 was used for synthesis of the anti-NAB1 antibody (SeqLab). Antisera were used in conjunction with the Amersham enhanced chemiluminescence system. LHCBM4/6-specific antibodies were raised against the synthetically produced 25 N-terminal amino acids of the LHCBM6 precursor protein (Hippler et al., 2001). Signals were quantified using the programs Quantity One (version 4.1.1; Bio-Rad) and GelScan 2.0.

MALDI-TOF and Electrospray Ionization Tandem Mass Spectrometry

MALDI-TOF mass spectrometry (Hillenkamp and Karas, 1990) was performed using a Bruker Biflex III apparatus and Xmass 5.0 software. For sample preparation, the Coomassie Brilliant Blue G 250–stained protein band of interest was cut out and treated according to the description at http://info.med.yale.edu/wmkeck/prochem/geldig3.htm. Acquisition of electrospray ionization tandem mass spectrometry data was achieved as described previously (Stauber et al., 2003).

Electron Microscopy

For transmission electron microscopy, cells were grown in TAP medium to an OD$_{750}$ of 0.6 and prepared as described (Engels et al., 1997).

In Vitro Synthesis of RNA and UV Cross-Linking of RNA with Proteins

Templates for the in vitro synthesis of the *LHCBM6* and *LHCBM4* cDNA probes were generated by PCR amplification using gene-specific oligonucleotides derived from the 5′ and 3′ UTRs.

Each template contained the T7 promoter sequence fused to the 5′ end of the appropriate fragment. In vitro transcription of RNA, UV cross-linking of RNAs with proteins, and quantification of binding signals were performed as described (Ossenbühl and Nickelsen, 2000). For competition experiments, radiolabeled RNA and nonlabeled competitor RNA were mixed before the addition of proteins.

Subpolysome and Polysome Complex Fractionation

Untranslated RNA in mRNPs and polysomes were fractionated as described (Barkan, 1988; Yohn et al., 1996). A cell lysate was layered onto a 15 to 45% sucrose gradient (Shama and Meyuhas, 1996). If desired, samples were pretreated with 500 μg/mL RNase A (Boehringer) for 5 min at 20°C. Collected fractions were supplemented with 0.5% (w/v) SDS and 20 mM EDTA before RNA extraction by phenol/chloroform extraction and isopropanol precipitation. Precipitated RNA was dissolved in 20 μL of dimethyldicarbonate-treated water, and 1 μL of each sample was separated on a 1.5% agarose-formaldehyde denaturing gel.

Immunoprecipitation of NAB1 and in Vivo RNA Binding Studies

A wild-type cell lysate was incubated with anti-NAB1 antiserum coupled to protein A–Sepharose (Seize classic immunoprecipitation kit; Pierce). Immunocomplexes were eluted according to the manufacturer's instructions, and RNA was isolated in the presence of 20 μg/mL glycogen. Coprecipitated RNA was subjected to real-time RT-PCR analysis with *LHCBM4*-, *LHCBM6*-, and *ACTIN*-specific primer pairs derived from the 3′ UTR using the QuantiTect SYBR Green RT-PCR kit in conjunction with the DNA Engine Opticon system (Bio-Rad).

Accession Number

The accession number for *NAB1* is AY157846.

REFERENCES

Allen, J.F. (1992). Protein phosphorylation in regulation of photosynthesis. Biochim. Biophys. Acta **1098,** 275–335.

Allen, J.F., and Forsberg, J. (2001). Molecular recognition in thylakoid structure and function. Trends Plant Sci. **6,** 317–326.

Allen, K.D., and Staehelin, L.A. (1991). Resolution of 16 to 20 chlorophyll protein complexes using a low ionic-strength native green gel system. Anal. Biochem. **194,** 214–222.

Anderson, S.L., and Kay, S.A. (1995). Functional dissection of circadian clock-regulated and phytochrome-regulated transcription of the Arabidopsis Cab2 gene. Proc. Natl. Acad. Sci. USA **92,** 1500–1504.

Barkan, A. (1988). Proteins encoded by a complex chloroplast transcription unit are each translated from both monocistronic and polycistronic mRNAs. EMBO J. **7,** 2637–2644.

Bonaventura, C., and Myers, J. (1969). Fluorescence and oxygen evolution from *Chlorella pyrenoidosa.* Biochim. Biophys. Acta **189,** 366–386.

Danon, A. (1997). Translational regulation in the chloroplast. Plant Physiol. **115,** 1293–1298.

Danon, A., and Mayfield, S.P. (1994). Light-regulated translation of chloroplast messenger RNAs through redox potential. Science **266,** 1717–1719.

Depege, N., Bellafiore, S., and Rochaix, J.D. (2003). Role of chloroplast protein kinase Stt7 in LHCII phosphorylation and state transition in Chlamydomonas. Science **299,** 1572–1575.

Drapier, D., Girard-Bascou, J., Stern, D.B., and Wollman, F.A. (2002). A dominant nuclear mutation in Chlamydomonas identifies a factor controlling chloroplast mRNA stability by acting on the coding region of the atpA transcript. Plant J. **31,** 687–697.

Durnford, D.G., and Falkowski, P.G. (1997). Chloroplast redox regulation of nuclear gene transcription during photoacclimation. Photosynth. Res. **53,** 229–241.

Durnford, D.G., Price, J.A., McKim, S.M., and Sarchfield, M.L. (2003). Light-harvesting complex gene expression is controlled by both transcriptional and post-transcriptional mechanisms during photoacclimation in *Chlamydomonas reinhardtii.* Physiol. Plant. **118,** 193–205.

Elrad, D., and Grossman, A.R. (2004). A genome's-eye view of the light-harvesting polypeptides of *Chlamydomonas reinhardtii.* Curr. Genet. **45,** 61–75.

Elrad, D., Niyogi, K.K., and Grossman, A.R. (2002). A major light-harvesting polypeptide of photosystem II functions in thermal dissipation. Plant Cell **14,** 1801–1816.

Engels, A., Kahmann, U., Ruppel, H.G., and Pistorius, E.K. (1997). Isolation, partial characterization and localization of a dihydrolipoamide dehydrogenase from the cyanobacterium Synechocystis PCC 6803. Biochim. Biophys. Acta **1340,** 33–44.

Escoubas, J.M., Lomas, M., Laroche, J., and Falkowski, P.G. (1995). Light-intensity regulation of Cab gene transcription is signaled by the redox state of the plastoquinone pool. Proc. Natl. Acad. Sci. USA **92,** 10237–10241.

Evdokimova, V., Ruzanov, P., Imataka, H., Raught, B., Svitkin, Y., Ovchinnikov, L.P., and Sonenberg, N. (2001). The major mRNA-associated protein YBA is a potent 5′ cap-dependent mRNA stabilizer. EMBO J. **20,** 5491–5502.

Finazzi, G., Barbagallo, R.P., Bergo, E., Barbato, R., and Forti, G. (2001). Photoinhibition of *Chlamydomonas reinhardtii* in state 1 and state 2—Damages to the photosynthetic apparatus under linear and cyclic electron flow. J. Biol. Chem. **276,** 22251–22257.

Finazzi, G., Furia, A., Barbagallo, R.P., and Forti, G. (1999). State transitions, cyclic and linear electron transport and photophosphorylation in *Chlamydomonas reinhardtii.* Biochim. Biophys. Acta **1413,** 117–129.

Fischer, N., and Rochaix, J.D. (2001). The flanking regions of PsaD drive efficient gene expression in the nucleus of the green alga *Chlamydomonas reinhardtii.* Mol. Genet. Genomics **265,** 888–894.

Flachmann, R., and Kühlbrandt, W. (1995). Accumulation of plant antenna complexes is regulated by posttranscriptional mechanisms in tobacco. Plant Cell **7,** 149–160.

Fleischmann, M.M., Ravanel, S., Delosme, R., Olive, J., Zito, F., Wollman, F.A., and Rochaix, J.D. (1999). Isolation and characterization of

photoautotrophic mutants of *Chlamydomonas reinhardtii* deficient in state transition. J. Biol. Chem. **274,** 30987–30994.

Graumann, P., and Marahiel, M.A. (1996). A case of convergent evolution of nucleic acid binding modules. Bioessays **18,** 309–315.

Graumann, P.L., and Marahiel, M.A. (1998). A superfamily of proteins that contain the cold-shock domain. Trends Biochem. Sci. **23,** 286–290.

Grossman, A. (2000). Acclimation of *Chlamydomonas reinhardtii* to its nutrient environment. Protist **151,** 201–224.

Harris, E.H. (1989). The Chlamydomonas Sourcebook: A Comprehensive Guide to Biology and Laboratory Use. (San Diego, CA: Academic Press).

Hillenkamp, F., and Karas, M. (1990). Mass-spectrometry of peptides and proteins by matrix-assisted ultraviolet-laser desorption ionization. Methods Enzymol. **193,** 280–295.

Hippler, M., Klein, J., Fink, A., Allinger, T., and Hoerth, P. (2001). Towards functional proteomics of membrane protein complexes: Analysis of thylakoid membranes from *Chlamydomonas reinhardtii.* Plant J. **28,** 595–606.

Imbault, P., Wittemer, C., Johanningmeier, U., Jacobs, J.D., and Howell, S.H. (1988). Structure of the *Chlamydomonas reinhardtii* CabII-1 gene encoding a chlorophyll-a/b-binding protein. Gene **73,** 397–407.

Jones, P.G., Vanbogelen, R.A., and Neidhardt, F.C. (1987). Induction of proteins in response to low temperature in *Escherichia coli.* J. Bacteriol. **169,** 2092–2095.

Kindle, K.L. (1990). High-frequency nuclear transformation of *Chlamydomonas reinhardtii.* Proc. Natl. Acad. Sci. USA **87,** 1228–1232.

Kruse, O., Nixon, P.J., Schmid, G.H., and Mullineaux, C.W. (1999). Isolation of state transition mutants of *Chlamydomonas reinhardtii* by fluorescence video imaging. Photosynth. Res. **61,** 43–51.

Lindahl, M., Yang, D.H., and Andersson, B. (1995). Regulatory proteolysis of the major light-harvesting chlorophyll a/b protein of photosystem II by a light-induced membrane-associated enzymatic system. Eur. J. Biochem. **231,** 503–509.

Lumbreras, V., Stevens, D.R., and Purton, S. (1998). Efficient foreign gene expression in *Chlamydomonas reinhardtii* mediated by an endogenous intron. Plant J. **14,** 441–447.

Manival, X., Ghisolfi-Nieto, L., Joseph, G., Bouvet, P., and Erard, M. (2001). RNA-binding strategies common to cold-shock domain- and RNA recognition motif-containing proteins. Nucleic Acids Res. **29,** 2223–2233.

Marco, Y., and Rochaix, J.D. (1980). Organization of the nuclear ribosomal DNA of *Chlamydomonas reinhardii.* Mol. Gen. Genet. **177,** 715–723.

Matsumoto, K., Meric, F., and Wolffe, A.P. (1996). Translational repression dependent on the interaction of the Xenopus Y-box protein FRGY2 with mRNA—Role of the cold shock domain, tail domain, and selective RNA sequence recognition. J. Biol. Chem. **271,** 22706–22712.

Matsumoto, K., Tanaka, K.J., Aoki, K., Sameshima, M., and Tsujimoto, M. (2003). Visualization of the reconstituted FRGY2-mRNA complexes by electron microscopy. Biochem. Biophys. Res. Commun. **306,** 53–58.

Maxwell, D.P., Laudenbach, D.E., and Huner, N.P.A. (1995). Redox regulation of light-harvesting complex II and Cab mRNA abundance in *Dunaliella salina.* Plant Physiol. **109,** 787–795.

Maxwell, K., and Johnson, G.N. (2000). Chlorophyll fluorescence—A practical guide. J. Exp. Bot. **51,** 659–668.

Millar, A.J., Straume, M., Chory, J., Chua, N.H., and Kay, S.A. (1995). The regulation of circadian period by phototransduction pathways in Arabidopsis. Science **267,** 1163–1166.

Moore, M.J. (2005). From birth to death: The complex lives of eukaryotic mRNAs. Science **309,** 1514–1518.

Murata, N. (1969). Control of excitation transfer in photosynthesis. Light-induced change of chlorophyll a fluorescence in *Porphyridium cruentum.* Biochim. Biophys. Acta **172,** 242–251.

Nelson, J.A.E., Savereide, P.B., and Lefebvre, P.A. (1994). The Cry1 gene in *Chlamydomonas reinhardtii*—Structure and use as a dominant selectable marker for nuclear transformation. Mol. Cell. Biol. **14,** 4011–4019.

Ossenbühl, F., and Nickelsen, J. (2000). cis- and trans-acting determinants for translation of psbD mRNA in *Chlamydomonas reinhardtii.* Mol. Cell. Biol. **20,** 8134–8142.

Petracek, M.E., Dickey, L.F., Huber, S.C., and Thompson, W.F. (1997). Light-regulated changes in abundance and polyribosome association of ferredoxin mRNA are dependent on photosynthesis. Plant Cell **9,** 2291–2300.

Petracek, M.E., Konkel, L.M.C., Kable, M.L., and Berman, J. (1994). A Chlamydomonas protein that binds single-stranded G-strand telomere DNA. EMBO J. **13,** 3648–3658.

Sambrook, J., Fritsch, E.F., and Maniatis, T. (1989). Molecular Cloning: A Laboratory Manual. (Cold Spring Harbor, NY: Cold Spring Harbor Laboratory Press).

Schönfeld, C., Wobbe, L., Borgstadt, R., Kienast, A., Nixon, P.J., and Kruse, O. (2004). The nucleus-encoded protein MOC1 is essential for mitochondrial light acclimation in *Chlamydomonas reinhardtii.* J. Biol. Chem. **279,** 50366–50374.

Shama, S., and Meyuhas, O. (1996). The translational cis-regulatory element of mammalian ribosomal protein mRNAs is recognized by the plant translational apparatus. Eur. J. Biochem. **236,** 383–388.

Shepherd, H.S., Ledoigt, G., and Howell, S.H. (1983). Regulation of light-harvesting chlorophyll-binding protein (Lhcp) mRNA accumulation during the cell cycle in *Chlamydomonas reinhardi.* Cell **32,** 99–107.

Stauber, E.J., Fink, A., Markert, C., Kruse, O., Johanningmeier, U., and Hippler, M. (2003). Proteomics of *Chlamydomonas reinhardtii* light-harvesting proteins. Eukaryot. Cell **2,** 978–994.

Stevens, D.R., Rochaix, J.D., and Purton, S. (1996). The bacterial phleomycin resistance gene ble as a dominant selectable marker in Chlamydomonas. Mol. Gen. Genet. **251,** 23–30.

Strauss, C., Mussgnug, J.H., and Kruse, O. (2001). Ligation-mediated suppression-PCR as a powerful tool to analyse nuclear gene sequences in the green alga *Chlamydomonas reinhardtii.* Photosynth. Res. **70,** 311–320.

Tang, L., Bhat, S., and Petracek, M.E. (2003). Light control of nuclear gene mRNA abundance and translation in tobacco. Plant Physiol. **133,** 1979–1990.

Teramoto, H., Nakamori, A., Minagawa, J., and Ono, T. (2002). Light-intensity-dependent expression of Lhc gene family encoding light-harvesting chlorophyll-a/b proteins of photosystem II in *Chlamydomonas reinhardtii.* Plant Physiol. **130,** 325–333.

Yang, D.H., Andersson, B., Aro, E.M., and Ohad, I. (2001). The redox state of the plastoquinone pool controls the level of the light-harvesting chlorophyll a/b binding protein complex II (LHC II) during photoacclimation—Cytochrome b(6)f deficient *Lemna perpusilla* plants are locked in a state of high-light acclimation. Photosynth. Res. **68,** 163–174.

Yohn, C.B., Cohen, A., Danon, A., and Mayfield, S.P. (1996). Altered mRNA binding activity and decreased translation initiation in a nuclear mutant lacking translation of the chloroplast psbA mRNA. Mol. Cell. Biol. **16,** 3560–3566.